Solar-Terrestrial Physics. 2021. Vol. 7. Iss. 3. P. 29–35. DOI: 10.12737/stp-73202103. © 2021 Makarov G.A. Published by INFRA-M Academic Publishing House. Original Russian version: Makarov G.A., published in Solnechno-zemnaya fizika. 2021. Vol. 7. Iss. 3. P. 31–38. DOI: 10.12737/szf-73202103. © 2021 INFRA-M Academic Publishing House (Nauchno-Izdatelskii Tsentr INFRA-M)

OFFSETS IN THE GEOMAGNETIC INDICES OF THE MAGNETOSPHERIC RING CURRENT

G.A. Makarov
Yu.G. Shafer Institute of Cosmophysical Research and Aeronomy SB RAS, Yakutsk, Russia, gmakarov@ikfia.ysn.ru
Yakut Scientific Centre of Siberian Branch of RAS, Yakutsk, Russia

Abstract. The paper considers changes in the daily average values of the *Dst*, *SYM-H*, *ASY-H*, and *ASY-D* indices and their dependence on the level of magnetic disturbance for the period 1981–2016. These indices are geomagnetic characteristics of the magnetospheric ring current. It has been established that the indices of the asymmetric component of the ring current *ASY-H* and *ASY-D* during relatively magnetically quiet periods are not equal to zero. The values of the offsets in the dependences of the *ASY-H* and *ASY-D* indices on the level of magnetic disturbance have been determined. The behavior of the index of the degree of symmetry of the ring current, the ratio *SYM-H*/*ASY-H*, is analyzed during the year at different levels of disturbance. This ratio has been found to grow in absolute value with increasing disturbance and to exceed 1 at large disturbances (at $Dst < -50$).

Keywords: geomagnetic index *Dst*, geomagnetic indices *SYM* and *ASY*, magnetospheric ring current.

INTRODUCTION

Ring current is an important part of Earth's magnetosphere. During magnetic storms, it is amplified during the main phase and returns to its original state during the recovery phase [Bazarzhapov et al., 1979]. Geomagnetic characteristics of the ring current are the *Dst*, *SYM*, and *ASY* indices: *Dst* reflects the ring current intensity [Sugiura, Kamei, 1991]; *SYM* and *ASY*, its symmetric and asymmetric components [Iyemori et al., 1992].

The *Dst* and *SYM*, *ASY* indices differ in temporal resolution and composition of ground networks of magnetic stations whose data is used to determine these indices: *Dst* has an hour temporal resolution; *SYM* and *ASY*, one-minute resolution; *Dst* is calculated from data on the geomagnetic field horizontal component *H* at four low-latitude stations, whereas *SYM* and *ASY* are subdivided into *SYM-H*, *SYM-D*, *ASY-H*, and *ASY-D* and are calculated from the geomagnetic field components *H* and *D* at six stations (the network consists of more than ten stations). It is noteworthy that *SYM-H* and *SYM-D* represent, in fact, averaged deviations of the *H* and *D* components from the quiet level at monitoring stations corrected for the geomagnetic latitude, while *ASY-H* and *ASY-D* are defined as ranges between maximum and minimum values of the *H* and *D* components after corresponding symmetric parts were subtracted from the disturbance field. *SYM-H* usually has negative values (like *Dst*); *SYM-D* takes values of both signs; *ASY-H* and *ASY-D* always have positive values. A method for determining *Dst* is described in detail in [Sugiura, Kamei, 1991]; *SYM* and *ASY*, in [Iyemori et al., 2010].

When studying *SYM*, *ASY*, and *Dst* variations, the authors of [Weygand, McPherron, 2006; Iyemori et al., 2010] have found that there are offsets in their values. According to the definition given in these papers, an offset is a non-zero index value under magnetically quiet conditions. The offsets were assumed to be the total contribution of the ring current and the magnetopause and magnetotail current systems existing in the magnetosphere during magnetically quiet periods.

Maltsev et al. [1996] proposed a formula for calculating *Dst*, which took into account contributions of the ring current, magnetopause currents, and transverse currents of the magnetotail. During quiet periods, contributions of these sources may be as great as tens of nanotesla. Kalegaev et al. [2005] have calculated the contributions made by ring, magnetotail, and magnetopause currents to *Dst*, using three models of the magnetospheric magnetic field: paraboloid, event-driven, and the Tsyganenko model T01. All the models show a significant contribution of the magnetotail current, comparable with that of the ring current during moderate magnetic storms.

From satellite measurements of ring current ions, Greenspan, Hamilton [2000] have found that magnetotail and magnetopause currents can induce strong magnetic disturbances, which should compensate the part of the ring current field, thereby creating ring current anisotropy during the day.

Statistical study of the effect of increasing solar wind dynamic pressure on the ring current asymmetry with the *ASY-H* index [Shi et al., 2006] has revealed an increase in the ring current asymmetry, which depends strongly on the north-south component of the interplanetary magnetic field. It was also shown that at mid-latitudes around the local noon or midnight the perturbations of *H* and hence *ASY-H* often include a significant contribution of field-aligned currents of both regions or that of the substorm current wedge.

Tsyganenko and Sitnov [2005], when developing a dynamic model of the geomagnetic field during a storm in the inner magnetosphere, took into account contributions of the main sources of the external magnetic field: magnetopause, transverse current sheet, axisymmetric and partial ring currents, and Birkeland current systems. Expected *Dst* variations were also calculated and compared with its actual values; the total correlation coefficient was over 0.92.

Dubyagin et al. [2014] using the empirical models of the magnetosphere, developed by N.A. Tsyganenko et

al., have studied relative contributions of various current systems to *SYM* and *ASY*. They have found that the symmetric ring current contribution to *SYM-H* begins to increase near the minimum value of *SYM-H* and reaches its peak during the storm recovery phase; the current across the magnetotail makes the main contribution to this index during the main phase. Dubyagin et al. [2014] point out, however, that this result should be treated with caution since model region 2 of field-aligned currents, the partial ring current, and transverse current systems overlap in the vicinity of the geostationary orbit, making it difficult to separate their effects. A good fit of real indices to those calculated by the magnetospheric models suggests that purely ionospheric current systems make, on average, a moderate contribution to these indices. Haiducek et al. [2017] using the SWMF system have modeled the forecast of the geomagnetic indices K_p, *SYM-H*, *AL* and has found that the model excels at forecasting the *SYM-H* index with a root-mean-square error 17–18 nT.

The ring current is an important structure in Earth's magnetosphere and plays a key role in the development of geomagnetic storms. The study of solar-terrestrial relations and manifestations of space weather will be incomplete without taking into account properties of the ring current. Such studies are often carried out by statistical methods using daily average terrestrial, interplanetary, and solar parameters. For daily averaged terrestrial parameters, different phases of geomagnetic storms may overlap; therefore, the storm parameters such as phase, intensity, duration, etc. will largely be smoothed over. Thus, it is important to examine variations in the daily average geomagnetic indices *Dst*, *SYM*, and *ASY*.

The purpose of this paper is to estimate offsets in *SYM-H*, *ASY-H*, and *ASY-D* from their daily average values.

1. EXPERIMENTAL MATERIAL

The paper uses the hourly average *Dst* index and one minute *SYM-H*, *SYM-D*, *ASY-H*, *ASY-D* indices for 1981–2016. The index values have been taken from the World Data Center for Geomagnetism, Kyoto, Japan [http: //wdc.kugi.kyoto-u.ac.jp / dstdir / index.html].

The relationship between daily average values of *Dst* and the planetary geomagnetic index A_p has been analyzed in our sample. The *Dst* modulus was found to be directly proportional to A_p. The relationship between these indices can be approximated by the linear equation $Dst=-1.39A_p+2.1$ when the approximation reliability value $R^2=0.987$; therefore, *Dst* is used hereinafter as a magnetic disturbance index. This approach allows us to see differences between the ring current indices considered.

In this paper, the indices are daily averaged on the universal time scale (UT). All data is divided into nine groups according to the average daily *Dst* index. Ranges of *Dst* variations, the number of days *N* in each group, as well as average *Dst* and A_p values in the groups are listed in Table 1.

The *SYM-D* index is omitted because, according to the preliminary analysis, when averaged over day and night it has small values, varies only occasionally during the year, and shows no dependence on the level of magnetic disturbance.

2. IDENTIFICATION OF OFFSETS IN *SYM-H*, *ASY-H*, AND *ASY-D*

Figure 1 shows seasonal variations in daily average values of *Dst*, *SYM-H*, *ASY-H*, and *ASY-D* in each disturbance group; variations for the 9th group are omitted due to the small number of days in it. It can be observed that *SYM-H*, *ASY-H*, and *ASY-D*, unlike *Dst*, vary a little during the year — grow in absolute value during summer months. We can also see their dependence on the level of magnetic disturbance: during disturbed periods these indices rise significantly in absolute value, and the amplitude of their annual variations increases as well. During relatively quiet periods, annual average *Dst*, *SYM-H*, *ASY-H*, and *ASY-D* are 2.8, 0.8, 14.4, and 13.7 nT respectively. The term "relatively quiet periods" is used in this study due to the fact that when the geomagnetic indices are daily averaged, in groups 1 and 2 there are days with magnetic disturbances lasting for several hours.

Table 1

Ranges of *Dst* variations, the number of days *N*, average *Dst* and A_p in groups of magnetic activity

Group of magnetic activity	Ranges of variations in *Dst*, nT	Number of days *N*	Average value of *Dst*, nT	Average value of A_p, nT
1	>0	2307	5.5	5.6
2	0	321	0	5.5
3	–10÷–1	3690	–5.5	7.1
4	–20÷–11	2941	–15.1	11.0
5	–30÷–21	1713	–25.0	16.5
6	–50÷–31	1464	–38.4	23.5
7	–100÷–51	608	–65.4	40.7
8	–150÷–101	81	–117.5	90.3
9	<–150	24	–180.3	132.3

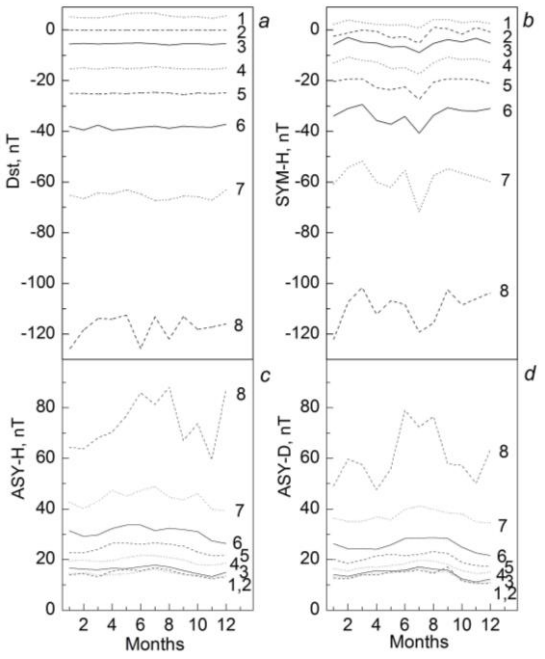

Figure 1. Seasonal variations in *Dst* (*a*), *SYM-H* (*b*), *ASY-H* (*c*), and *ASY-D* (*d*) for some groups of magnetic disturbance

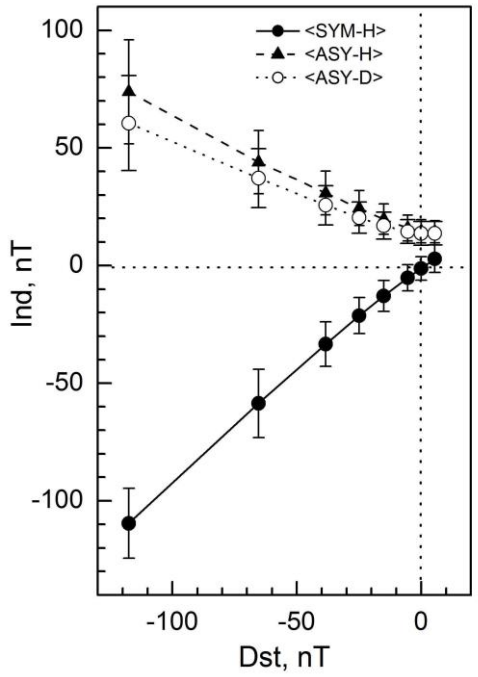

Figure 2. Variations in annual average *SYM-H*, *ASY-H*, and *ASY-D* as a function of average *Dst* in disturbance groups and their standard deviations. Dotted lines indicate zero *SYM-H*, *ASY-H*, *ASY-D*, and *Dst*

Figure 2 illustrates variations in annual average *SYM-H*, *ASY-H*, and *ASY-D* as a function of annual average *Dst* separately for disturbance groups. All the annual average indices exhibit an almost linear dependence on *Dst*, with *SYM-H* increasing with *Dst* nearly twice as great as the others. The *ASY-H* and *ASY-D* indices have the same offsets, equal to ~13 nT. There is a deviation from the linear dependence when *Dst*>0 and *Dst*=0. Parameters of the linear regression between *SYM-H*, *ASY-H*, *ASY-D* and *Dst*, and the linear approximation reliability values R^2 are given in Table 2 in row A (see below in Section 3). Note that R^2 are very high. Free terms *b* in the approximation equations determine values of the offsets.

Figure 3 shows daily average *SYM-H* (*a*), *ASY-H* (*b*), and *ASY-D* (*c*) as a function of daily average *Dst*. The plots were constructed using data for the entire period. The relationships are seen to be very close, *SYM-H* in modulus, as well as *ASY-H* and *ASY-D*, increases with the *Dst* modulus, which may be interpreted as a simultaneous increase in symmetric and asymmetric ring current components with increasing level of magnetic disturbance. It is noticeable that the symmetric component increases more dramatically than the asymmetric one. The relations between the indices can be approximated by the equations $SYM\text{-}H=0.86Dst-0.60$ with a linear approximation reliability value $R^2=0.88$, $ASY\text{-}H=-0.43Dst+14.40$ with $R^2=0.61$, and $ASY\text{-}D=-0.3252Dst+13.31$ with $R^2=0.51$; correlation coefficients between the pairs of indices are 0.94, –0.78, and –0.71 respectively. Similar distributions have been considered for negative *Dst* values; in this case, the relationship between the pairs of indices can also be approximated by the linear equations whose parameters are listed in Table 2 in row C.

Note that in the cases of *ASY-H* (*b*) and *ASY-D* (*c*) in Figure 3, as in Figure 2, there are offsets; and the approximation equations contain free terms: 14.4 nT in the pair *ASY-H* and *Dst* and 13.3 nT in the pair *ASY-D* and *Dst*. If we compare values of these offsets with the data from Figure 2, we can see that they are close.

These plots have been constructed for each group of *Dst* values. It has been found that in each group within respective *Dst* variations all the three indices show a fairly wide spread; however, there is a tendency for their moduli to increase linearly with the *Dst* modules. Results of the linear approximation of the *Dst* dependence of the three indices for each group are presented in Figure 4 as changes in regression coefficients *a* and free terms *b* as a function of average *Dst* in the magnetic disturbance groups. For the group *Dst*=0, the value of a particular index average for this sample is taken as the parameter *b* (see Table 2, row D).

Figure 4 demonstrates that the coefficient *a* for *SYM-H* increases with magnetic disturbance, but it varies in a small range of values (from 0.7 to 1.1) and thus indicates that *Dst* and *SYM-H* are close; under strong disturbance, their daily average values become almost equal. For *ASY-H* and *ASY-D*, the coefficient *a* is negative, except for group 1 (0 <*Dst*), and varies within fairly narrow limits relative approximately to –0.5 and –0.4 respectively. This means that the values of the indices are positive and almost twice as small as the *Dst* modulus. The parameter *b* exhibits a sufficiently pronounced dependence on *Dst* for *ASY-H* (panel *d*): it decreases with increasing *Dst* modulus. For *SYM-H* (panel *b*) and *ASY-D* (panel *f*), the parameter *b* shows an increase with increasing disturbance. The linear dependence of *b* on *Dst* can be approximated by the equation $b=a_2Dst+b_2$. The free terms b_2 of the equations derived are listed in Table 2, row E.

Table 2

Regression coefficients *a* and free terms *b* in equations approximating the *Dst* dependence of three indices, and approximation reliability values R^2

	Method of determining offsets	*SYM-H*			*ASY-H*			*ASY-D*		
		a	*b*, nT	R^2	*a*	*b*, nT	R^2	*a*	*b*, nT	R^2
A	From annual average Indices in *Dst* groups (Figure 2)	0.92	0.01	0.998	–0.49	13.61	0.99	–0.39	12.51	0.99
B	Linear approximation between the indices and *Dst* (all days (Figure 3))	0.86	–0.60	0.88	–0.43	14.40	0.61	–0.33	13.31	0.51
C	Linear approximation between the indices and *Dst* (days with *Dst*<0)	0.89	0.46	0.87	–0.48	12.86	0.62	–0.37	11.76	0.55
D	Averaging approximation coefficients over all *Dst* groups (Figure 4)	0.84	–0.34		–0.41	11.22		–0.32	12.49	
E	Free terms b_2 of linear regression of *b* dependence on *Dst* (Figure 4)		–1.14			14.43			11.12	
F	Annual average indices for *Dst*>0 and *Dst*=0 (Figure 1)		0.8			14.4			13.7	
G	Assessed value of *b* in terms of median and average values of *b*, obtained by different methods		–0.1			14			13	

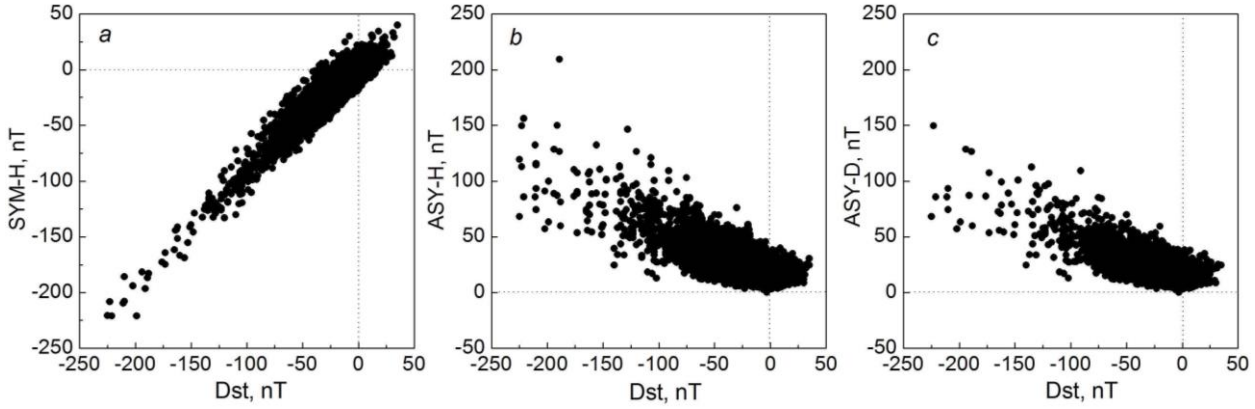

Figure 3. Correlation plots of daily average *SYM-H* (*a*), *ASY-H* (*b*), and *ASY-D* (*c*) for the entire data set. Dotted lines indicate zero *Dst*, *SYM-H*, *ASY-H*, and *ASY-D*

3. DISCUSSION

We have determined regression coefficients and free terms in linear approximation equations and offset values for three indices by six methods: from their annual average values in *Dst* groups (see Figure 2); when considering the regression for all days (see Figure 3); when considering the regression on days with *Dst*<0; in the form of average *b*, obtained separately for the disturbance groups (Figure 4); as free terms in equations for regression of the dependence of parameters *b* themselves on *Dst* (Figure 4); from annual average indices for *Dst*>0 and *Dst*=0 (Figure 1). The regression coefficients and the free terms in equations for approximation of the *Dst* dependence of three indices are listed in Table 2.

Consider the behavior of the free terms *b* (rows B–E), as well as annual average values of the indices (rows A and F). In this paper, the annual average values of the indices for *Dst*>0 and *Dst*=0 with an assumption can be taken as offsets. As seen from Table 2, the *b* values for *SYM-H* are small and vary around zero. For *ASY-H* and *ASY-D*, they are of the same order and range from 11.1 to 14.4 nT.

Given the median and mean values of the parameter *b*, obtained by different methods (Table 2, row G), we can estimate offset values for the three indices: –0.1 nT for *SYM-H*, 14 nT for *ASY-H*, and 13 nT for *ASY-D*.

From daily averaged geomagnetic indices it is impossible to find causes of the offsets. According to [Weygand, McPherron, 2006], which addresses one-minute

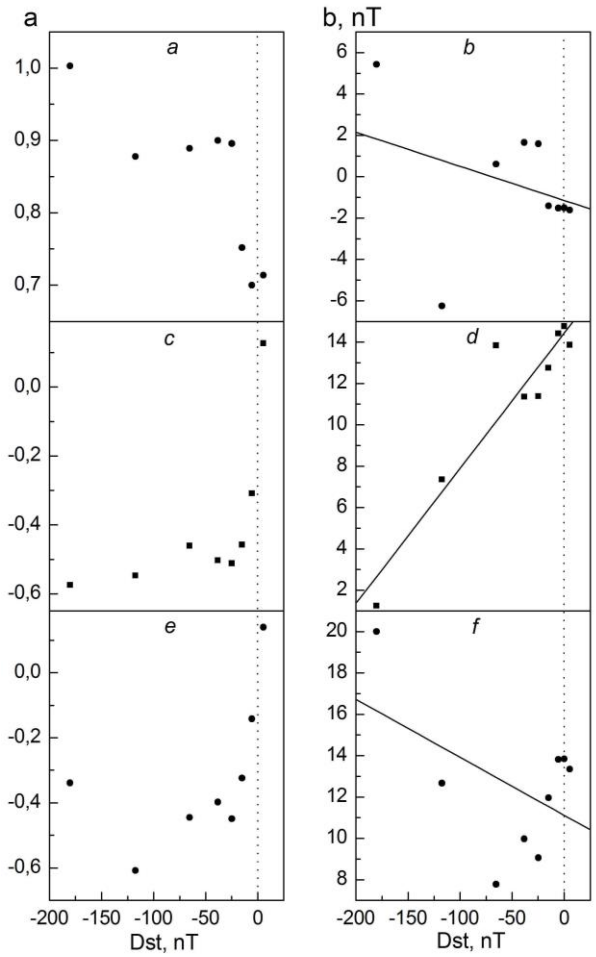

Figure 4. Distribution of regression coefficients *a* and free terms *b* of linear approximation equations for *SYM-H* (*a*, *b*), *ASY-H* (*c*, *d*), *ASY-D* (*e*, *f*) as a function of *Dst* in disturbance groups; straight solid lines are approximations for each of the three indices; vertical dotted lines mark *Dst*=0 nT

index values, the offset in *SYM-H* is likely to be caused by a combination of contributions of Chapman—Ferraro and ring currents under quiet conditions, as well as by the difference between contributions of magnetotail currents under quiet and disturbed conditions. Offsets in *ASY-H* are due to two causes: asymmetric ring current inherent in the inner magnetosphere and noise in data caused by incomplete subtraction of quiet day variation at each station. Jorgensen et al. [2004] have found that the ring current is asymmetric for all *Dst* values, and the azimuth ring current peak is located in the daytime sector for quiet conditions and near midnight for disturbed conditions. Using the dynamic model of Earth's magnetosphere, Alexeev et al. [1996] determined the contribution of the magnetotail current system to *Dst* variations during magnetic disturbances. From model and experimental studies of substorms during geomagnetic storms when *Dst* was around –80 nT, Turner et al. [2000] have found that the magnetotail current contribution is 22–26 nT; and for isolated substorms they have obtained an almost linear relationship between *Dst* and the magnetotail current contribution, which is about a quarter of *Dst*. Dubyagin et al. [2014], using data from comparison of model magnetospheric calculations with real indices, have established that the current systems completing through the ionosphere — the partial ring current and field-aligned current regions 1 and 2 — make a significant contribution to *ASY-H* and *ASY-D*.

Offsets in *Dst* values were also revealed. Mursula and Karinen [2005] have shown that due to seasonal variations in the magnetic field at *Dst* stations and due to incorrect processing of the quiet time curve when plotting the index a non-storm component appears in *Dst* variations. Hakkinen et al. [2003] have demonstrated that the average *Dst* levels differ approximately by 10 nT due to the fact that *Dst* stations have different baselines; to eliminate the secular variation, the authors have proposed a new method capable of changing the seasonal variation in *Dst* by ~3 nT. The model of forecasting *Dst* [Temerin, Li, 2006] assumes that the annual variation in *Dst* is mainly linked to magnetopause currents and ring currents, as well as to the location of magnetometer stations, used to calculate *Dst*. Makarov [2020] has shown the annual *Dst* variation occurs due to the nonuniform distribution of the network of stations involved in determining *Dst*.

Let us delve into such a characteristic as the ring current symmetry ratio *SYM-H*/*ASY-H* [Weygand, McPherron, 2006]. Figure 5 illustrates seasonal variations in the ratio *SYM-H*/*ASY-H* for different values of *Dst*, obtained from daily average values of the indices. Note that when effects of all storm phases as well as the effects of quiet periods are daily averaged, the ring current symmetry ratio is largely meaningless; however, qualitative conclusions can be drawn.

Figure 5 demonstrates the following features: first, during periods when *Dst*>0 the ratio *SYM-H*/*ASY-H* is positive; second, during periods when *Dst*>–20 nT, the absolute value of *SYM-H*/*ASY-H* is less than 1; third, this ratio increases in absolute value with the level of magnetic disturbance; fourthly, during strong disturbances (when *Dst*<–50) the absolute value of the ratio exceeds 1 and approaches 2.

The first feature can be explained by the fact that under conditions when *Dst*>0, *SYM-H* also has positive values as an analogue of the *Dst* index. The second feature may represent the evidence for the presence of an offset, obtained when considering *ASY-H* variations in Figures 1–4. The third feature indicates a gradual increase in the symmetric ring current component relative to the asymmetric component as the magnetic disturbance level goes up. A fourth feature suggests the predominance of the symmetric ring current component during highly disturbed periods. The last two characteristics can probably be explained by the use of daily average data: since the storm recovery phase is much longer (about three times or more) than the main phase, the symmetric ring current persists for a longer time and, when daily averaged, makes a contribution to geomagnetic variations, which exceeds the contribution of the asymmetric ring current component during the main phase when this current is much stronger. It is known [Weygand, McPherron, 2006], for example, that the response time for *SYM-H* (5.25 and 64.3 hr) is almost twice as long as that for *ASY-H* (2.2 and 20.9 hrs).

Suppose that during relatively quiet periods there are no magnetospheric current systems that create an offset in *ASY-H*. From the data in Figure 2, which shows annual average *ASY-H*, subtract 13.6 nT — the offset in this index (parameter *b* for *ASY-H* in Table 2, row A). Then, define the ratio *SYM-H* /*ASY-H* after considering the offset in *ASY-H*. Figure 6 shows the *SYM-H*/*ASY-H* ratio, obtained from annual average values of the indices, presented in Figure 2 (curve 1), and from the same data but with correction for the offset in *ASY-H* (curve 2), as the dependence on average *Dst*

In Figure 6, curve 1 behaves as described according to data from Figure 5; and curve 2, in a different way: in all the disturbance groups, relations in absolute value are greater than 1; and in groups 3–8, even near 2. This suggests that during relatively quiet periods and at a low level of disturbance the consideration of the offset in *ASY-H* reflects the predominance of the symmetric ring current component over the asymmetric one. With increasing disturbance level, the symmetric component increases twice as great as the asymmetric one (this can be seen in Figures 2, 3), and this is shown in Figure 6 as a plateau at

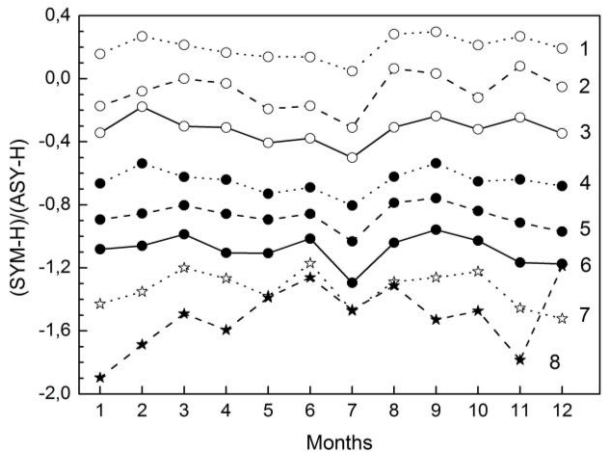

Figure 5. Behavior of the ring current symmetry ratio *SYM-H*/*ASY-H* during the year. Numbers denote magnetic disturbance groups

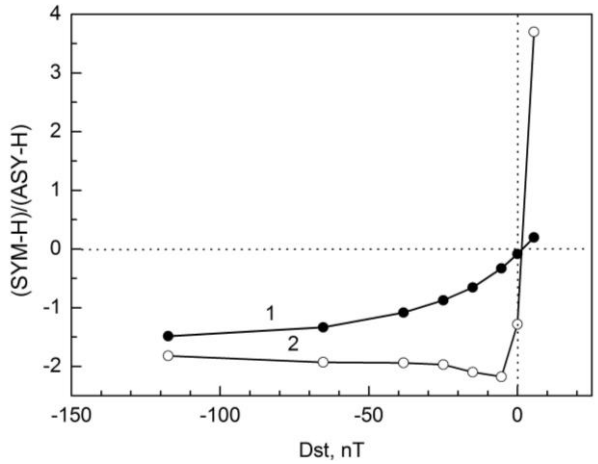

Figure 6. Relationship between *Dst* and the ring current symmetry ratio *SYM-H*/*ASY-H* obtained from the annual average values of the indices in magnetic disturbance groups (curve 1) and from the same data, but with correction for the offset in *ASY-H* (curve 2). Dotted lines mark zero values of *Dst* and *SYM-H*/*ASY-H*

medium and high levels of disturbance. Furthermore, this ratio of the indices confirms the explanation of the third and fourth features, pointed out when discussing Figure 5: when daily averaged, due to the fact that the storm recovery phase is much longer than the main phase, the symmetric ring current component makes a greater contribution to *SYM-H* than the asymmetric one to *ASY-H*.

4. MAIN RESULTS

1. It has been shown that the daily average values of the magnetospheric ring current geomagnetic indices *SYM-N*, *ASY-H*, and *ASY-D* feature seasonal variations and depend on the level of magnetic disturbance — absolute values of all the indices go up in summer months and linearly increase with disturbance, which may be interpreted as simultaneous amplification of the symmetric and asymmetric ring current components in the magnetosphere; the symmetric component increasing more dramatically than the asymmetric one.

2. From data on seasonal variations it has been found that the geomagnetic indices of the asymmetric magnetospheric ring current component *ASY-H* and *ASY-D* during relatively quiet periods are not equal to zero: their annual average values are 14.4 and 13.7 nT respectively.

3. From the results of the regression analysis of daily average *ASY-H*, *ASY-D*, and *Dst* values, the offsets in the relationships of *ASY-H* and *ASY-D* with the level of magnetic disturbance, determined by *Dst*: 14.4 nT for *ASY-H*, 13.3 nT for *ASY -D*, have been identified.

4. From daily average *SYM-H* and *ASY-H* values it has been found that the ring current symmetry ratio *SYM-H*/*ASY-H* grows in absolute value with increasing disturbance level, and during strong disturbances (when *Dst*<–50) it is greater than 1, which may be interpreted as a gradual increase in the symmetric magnetospheric ring current component with increasing level of disturbance and its dominance over the asymmetric component during strong disturbances.

The work was carried out in the framework of Government Assignment (State Registration Number AAAA A21-121012000007-4).

REFERENCES

Alexeev I.I., Belenkaya E.S., Kalegaev V.V., Feldstein Y.I., Grafe A. Magnetic storms and magnetotail currents. *J. Geophys. Res.* 1996, vol. 101, no. A4, pp. 7737–7747. DOI: 10.1029/95JA03509.

Bazarzhapov A.D., Matveev M.I., Mishin V.M. *Geomagnitnye variatsii i buri* [Geomagnetic Variations and Storms]. Novosibirsk, Nauka Publ., 1979, 248 p. (In Russian).

Dubyagin S., Ganushkina N., Kubyshkina M., Liemohn M. Contribution from different current systems to *SYM* and *ASY* midlatitude indices. *J. Geophys. Res.* 2014, vol. 119, pp. 7243–7263. DOI: 10.1002/2014JA020122.

Greenspan M.E., Hamilton D.C. A test of the Dessler-Parker-Sckopke relation during magnetic storms. *J. Geophys. Res.* 2000, vol. 105, no. A3, pp. 5419–5430. DOI: 10.1029/1999JA000284.

Haiducek J.D., Welling D.T., Ganushkina N.Y., Morley S.K., Dogacan Su Ozturk. SWMF global magnetosphere simulations of January 2005: Geomagnetic indices and cross-polar cap potential. *Space Weather*. 2017, vol. 15, pp. 1567–1587. DOI: 10.1002/

2017SW001695.

Hakkinen L.V.T., Pulkkinen T.I., Pirjola R.J., Nevanlinna H., Tanskanen E.I., Turner N.E. Seasonal and diurnal variation of geomagnetic activity: Revised *Dst* versus external drivers. *J. Geophys. Res.* 2003, vol. 108, iss. A2, 1060. DOI: 10.1029/2002JA009428.

Iyemori T., Araki T., Kamei T., Takeda M. Mid-latitude geomagnetic indices *ASY* and *SYM* (Provisional) No. 1 (1989–1990). *Internal Report of Data Analysis Center for Geomagnetism and Space Magnetism*. Kyoto University, Japan, 1992.

Iyemori T., Takeda M., Nose M., Odagi Y., Toh H. Mid-latitude geomagnetic indices "*ASY*" and "*SYM*" for 2009 (Provisional). *Internal Report of Data Analysis Center for Geomagnetism and Space Magnetism*. Kyoto University, Japan, 2010. Available at http://wdc.kugi.kyoto-u.ac.jp/aeasy/asy.pdf (accessed October 5, 2020).

Jorgensen A.M., Spence H.E., Hughes W.J., Singer H.J. A statistical study of the global structure of the ring current. *J. Geophys. Res.* 2004, vol. 109, A12204. DOI: 10.1029/2003JA010090.

Kalegaev V.V., Ganushkina N.Y., Pulkkinen T.I., Kubyshkina M.V., Singer H.J., Russell C.T. Relation between the ring current and the tail current during magnetic storms. *Ann. Geophys.* 2005, vol. 23, pp. 523–533. DOI: 10.5194/angeo-23-523-2005.

Makarov G.A. Geometric factor in seasonal variations of daily average values of the geomagnetic index *Dst*. *Solar-Terr. Phys*. 2020, vol. 6, iss. 4, pp. 50–56. DOI: 10.12737/stp-64202008.

Maltsev Y.P., Arykov A.A., Belova E.G., Gvozdevsky B.B., Safargaleev V.V. Magnetic flux redistribution in the storm time magnetosphere. *J. Geophys. Res*. 1996, vol. 101, no. A4, pp. 7697–7704. DOI: 10.1029/95JA03709.

Mursula K., Karinen A. Explaining and correcting the excessive semiannual variation in the *Dst* index. *Geophys. Res. Lett.* 2005, vol. 32, L14107. DOI: 10.1029/2005GL023132.

Shi Y., Zesta E., Lyons L.R., Yumoto K., Kitamura K. Statistical study of effect of solar wind dynamic pressure enhancements on dawn-to-dusk ring current asymmetry. *J. Geophys. Res.* 2006, vol. 111, A10216. DOI: 10.1029/2005JA011532.

Sugiura M., Kamei T. Equatorial *Dst* index 1957–1986. *IAGA Bull.* 1991, no. 40, 14 p.

Temerin M., Li X. *Dst* model for 1995–2002. *J. Geophys. Res.* 2006, vol. 111, A04221. DOI: 10.1029/2005JA011257.

Tsyganenko N.A., Sitnov M.I. Modeling the dynamics of the inner magnetosphere during strong geomagnetic storms. *J. Geophys. Res.* 2005. vol. 110, A03208. DOI: 10.1029/2004JA010798.

Turner N.E., Baker D.N., Pulkkinen T.I., McPherron R.L. Evaluation of the tail current contribution to *Dst*. *J. Geophys. Res.* 2000, vol. 105, no. A3, pp. 5431–5439. DOI: 10.1029/1999JA000248.

Weygand J.M., McPherron R.L. Dependence of ring current asymmetry on storm phase. *J. Geophys. Res.* 2006, vol. 111, A11221. DOI: 10.1029/2006JA011808.

URL: http://wdc.kugi.kyoto-u.ac.jp/dstdir/index.html (accessed October 5, 2020).

How to cite this article

Makarov G.A. Offset in the geomagnetic indices of the magnetospheric ring current. *Solar-Terrestrial Physics.* 2021. Vol. 7, Iss. 3. P. 29–35. DOI: 10.12737/stp-73202103.